

Electrical and thermoelectrical transport in Dirac fermions through a quantum dot

Tomosuke Aono¹

¹*Department of Electrical and Electronic Engineering, Ibaraki University, Hitachi 316-8511, Japan**
(Dated: September 3, 2012)

We investigate the linear conductance and the thermopower through a quantum dot between two electrodes of Dirac fermions with a pseudogap Anderson model using the non-crossing approximation. When the Fermi level is at the Dirac point, the conductance shows a valley, where the thermopower changes its sign. The conductance shows a peak when the Fermi level away from the Dirac point, where the impurity moment changes sharply, indicating a transition between an asymmetric strong coupling Kondo state and a localized moment state. The thermopower changes its sign in the vicinity of the peak. The magnitude of the thermopower can be more than k_B/e .

PACS numbers: 73.63.-b, 72.10.Fk, 85.80.Fi, 72.80.Vp

Electron transport in graphene [1] is currently under active investigation. Graphene-based quantum dot (QD) structure is fabricated and the Coulomb blockade effect is observed [2–5]. In semiconductor QD systems, it is known that the Coulomb interaction in the QD induces a magnetic moment, leading to the Kondo effect [6, 7]. The Kondo effect in graphene has been intensively discussed from the view of the magnetic impurity problem in massless Dirac fermions [8–14]. A recent experiment shows the Kondo effect can be induced by lattice vacancies [15]. The Kondo effect is expected to be observed in another representative Dirac fermions, the surface states of the topological insulator. A single Dirac cone appears on the surface of three dimensional topological insulators [16–20]. Several theoretical studies on the Kondo effect in this system have been developed [21–24].

The Kondo problem in massless Dirac fermions is an important part of the pseudogap Kondo problem [25], where the density of states of conduction electrons is proportional to ω^r with the energy of the electrons ω and an index r . It is for example realized in unconventional superconductors [25, 26]. The numerical renormalization calculations [27, 28] and perturbative scaling analyses [29, 30] show the system exhibits an impurity quantum phase transition. The massless Dirac fermion system corresponds to $r = 1$. In this case, when the Coulomb interaction is strong enough, three fixed points control the electronic states in the system, namely the local moment (LM) fixed point, the asymmetric strong coupling (ASC) or frozen impurity fixed point, and the valence fluctuation (VFI) fixed point located in between [27, 29, 30]. The Kondo problem in graphene has been studied as a tunable pseudogap Kondo problem [8, 13], where the transition can be controlled by external gate voltages. Recently the Kondo effect found in Ref. [15] has been analyzed using a pseudogap Anderson model [31].

In addition to electric transport, thermoelectric transport in nano-structures has been actively investigated

[32]. For instance, the measurement of the thermopower can reveal the electron-hole asymmetry in a system. The thermopower under the Kondo effect [33] has been examined in QD systems [34, 35]. In the QD system, its measurement clarifies the formation of the Kondo resonant state [36].

We investigate electric and thermoelectric transports through a QD between two electrodes of Dirac fermions. The tunneling coupling between the QD and the electrode is proportional to ω . We show how this pseudogap coupling controls electronic states of the system and the transport properties. In addition, we show how the impurity quantum phase transition influences those properties. To this end, we study the conductance, the thermopower and the impurity magnetic susceptibility based on a pseudogap Anderson model using the non-crossing approximation (NCA) [37–40].

Model. — We consider a system consisting of a QD and two electrodes with the Dirac fermions, as shown in the inset of Fig. 1(a). We treat the case of a single Dirac cone with the chemical potential μ_i ($i = L, R$), and focus on the zero bias voltage limit, $\mu_L \rightarrow \mu_R$, setting $\mu_i = 0$. The position of the Dirac point from the Fermi level is denoted by $-\mu_0$.

The Hamiltonian of Dirac fermions in the lead i , $H_0^{(i)}$ is given by

$$H_0^{(i)} = \int \frac{d^2k}{(2\pi)^2} (\Psi_a^\dagger(\mathbf{k}), \Psi_b^\dagger(\mathbf{k})) M(\mathbf{k}) \begin{pmatrix} \Psi_a(\mathbf{k}) \\ \Psi_b(\mathbf{k}) \end{pmatrix} \quad (1)$$

with $M(\mathbf{k}) = \begin{pmatrix} -\mu_0 & \hbar v_F k e^{-i\theta} \\ \hbar v_F k e^{i\theta} & -\mu_0 \end{pmatrix}$, where $\Psi_a(\mathbf{k})$ are the annihilation operators of Dirac fermions, v_F is the Fermi velocity, $\mathbf{k} = (k \cos \theta, k \sin \theta)$ with $k = |\mathbf{k}|$ and θ stands for the azimuth angle of \mathbf{k} from the x axis. The indexes a and b refer to (pseudo) spin indexes. For a single Dirac cone system, those are the spin indexes; $a = \uparrow$ and $b = \downarrow$. For graphene, $a = (A, s)$ and $b = (B, s)$ with the two sublattices A and B , which play the role of the pseudo spin, and the spin index $s = \uparrow, \downarrow$ around the K and K' points [41].

The QD has a single energy level E_g controlled by a

* aono@mx.ibaraki.ac.jp

gate voltage. The Hamiltonian for the QD is given by

$$H_d = \sum_{s=\uparrow,\downarrow} E_g d_s^\dagger d_s + U n_\uparrow n_\downarrow, \quad (2)$$

where d_s is the annihilation operator of an electron with spin s in the QD, $n_s = d_s^\dagger d_s$, and U is the Coulomb energy in the QD. The tunneling coupling between the QD and the lead is given by the tunneling Hamiltonian H_T , $H_T = \sum_{i=L,R,s} \int \frac{d^2 k}{(2\pi)^2} (V_i(\mathbf{k}) d_s^\dagger \Psi_s(\mathbf{k}) + \text{h.c.})$. For simplicity, we assume $V_i(\mathbf{k}) = V$.

It has been shown the QD with an electrode of Dirac fermions reduces to the pseudogap Anderson model after a series of linear transformations [8, 23, 26]. Then H_0 in the energy space is given by

$$H_0 = \sum_{i=L,R} \int d\omega \omega c_{\sigma i}^\dagger(\omega) c_{\sigma i}(\omega), \quad (3)$$

where $c_{\sigma i}(\omega)$ is the annihilation operator for an electron in the lead i with the pseudo spin index σ at the energy ω . The tunneling Hamiltonian H_T is given by

$$H_T = \sum_{i,\sigma} \int d\omega \sqrt{\Gamma(\omega)} d_\sigma^\dagger c_{\sigma i}(\omega) + \text{h.c.} \quad (4)$$

We have disregarded the difference between the spin and pseudo spin indexes, both are now represented by σ . The tunneling coupling between the dot and electrodes is $\Gamma(\omega) = \alpha(\omega + \mu_0)$ with $\alpha = \frac{V^2}{2\pi(\hbar v_F)^2}$ [10, 23, 24]. It is necessary to introduce an energy cut-off D , and then it is convenient to rewrite $\Gamma(\omega)$ in the form:

$$\Gamma(\omega) = \Gamma_0 \left| \frac{\omega + \mu_0}{D} \right| \quad (5)$$

with $\Gamma_0/D = \alpha$. The pseudogap Anderson model with $H = H_d + H_T + H_0$ is analyzed below.

We consider the infinite U model. This corresponds to the asymmetric pseudogap Anderson model [27, 29, 30]. We use the auxiliary boson technique [37, 42], where $d_\sigma = b^\dagger f_\sigma$, b is a boson operator and f_σ is a fermion operator; $b^\dagger b + \sum_\sigma f_\sigma^\dagger f_\sigma = 1$ should be satisfied. Then we adopt the NCA [37–40] to calculate the local density of states of the QD and other quantities. To perform the numerical calculations, we evaluate the Green functions on the range of $|\omega| \leq 10D$ and introduce the Lorentzian cut-off in the pseudogap coupling; $\Gamma_L(\omega) = \Gamma(\omega) \cdot D^2/(\omega^2 + D^2)$. The convergence of the NCA equations is monitored by the unity of the spectral functions for f_σ and b , and the relation on the total occupancy in the QD [39], which are satisfied typically with the accuracy of less than 0.1%.

The conductance G and the thermopower S are given by $G = e^2 I_0(T)$ and $S = -I_1(T)/[eT I_0(T)]$ with

$$I_n(T) = -2/h \int d\omega \omega^n \frac{\partial f(\omega)}{\partial \omega} \Gamma(\omega) \text{Im} A^r(\omega), \quad (6)$$

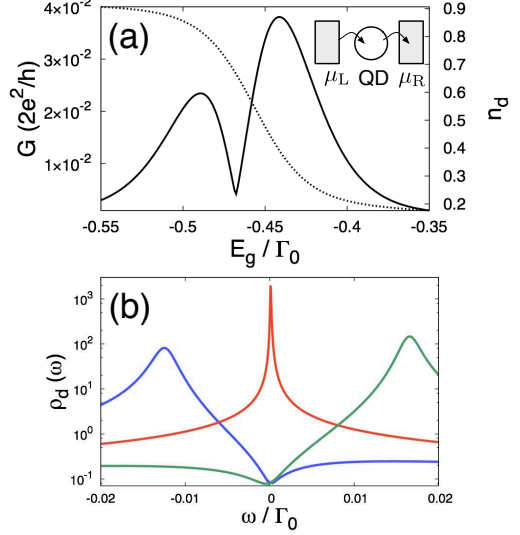


FIG. 1. Electron transport through a quantum dot (QD) between two electrodes of Dirac fermions when $\mu_0 = 0$. (a) Conductance G (solid line) and occupation number in the QD n_d (dotted line) as a function of gate voltage E_g for $T/\Gamma_0 = 1.0 \times 10^{-2}$, and $D/\Gamma_0 = 10$ ($\alpha = 0.1$). Inset (a): Schematic picture of the QD system. (b) Local density of states $\rho_d(\omega)$ at the left peak (blue), the cusp (red), and the right peak (green) in Fig. 1(a).

where $f(\varepsilon)$ is a Fermi-Dirac function, $f(\omega) = 1/[\exp(\frac{\omega}{k_B T}) + 1]$, and $A^r(\omega)$ is the retarded Green function for electrons in the QD [35, 43]. The impurity magnetic susceptibility $\chi(\omega)$ is given by $\chi(\omega) = \int_{-\infty}^{\infty} dt e^{i(\omega + i0^+)t} M(t)$ with $M(t) = i\theta(t)\langle[\hat{M}(t), \hat{M}(0)]\rangle$, and $\hat{M} = g\mu_B/2 (f_\uparrow^\dagger f_\uparrow - f_\downarrow^\dagger f_\downarrow)$. The static susceptibility $\chi = \chi(0)$ is evaluated using NCA [38]. We set $g\mu_B = 1$ and $k_B = 1$ below.

Undoped system.— Let us first consider G and the occupation number in the QD, n_d when the Fermi level is at the Dirac point; $\mu_0 = 0$. It has been shown that for this case, the Kondo temperature $T_K = 0$ [8, 13, 25]. In Fig. 1(a), G and n_d are plotted as a function of the gate voltage E_g . The plot of G shows a valley; $G \propto |E_g - E_g^*| + G_m$ with the minimum conductance G_m at the cusp, where $E_g = E_g^*$. Out of the valley, G decreases monotonically, consisting of double peaks. In the valley, n_d changes gradually. This means the system is in the VFI regime.

In Fig. 1(b), the density of states of the QD, $\rho_d(\omega) = (-1/\pi)\text{Im} A^r(\omega)$, is plotted. At $E_g = E_g^*$, $\rho_d(\omega)$ shows a narrow and singular peak at the Fermi level, $\omega = 0$. The appearance of such a distinct peak has been discussed [13, 28, 29]. In spite of this sharp peak of $\rho_d(\omega)$, G remains small because $\Gamma(\omega)$ suppresses the peak height.

In Fig. 2, G and the thermopower S are plotted as a

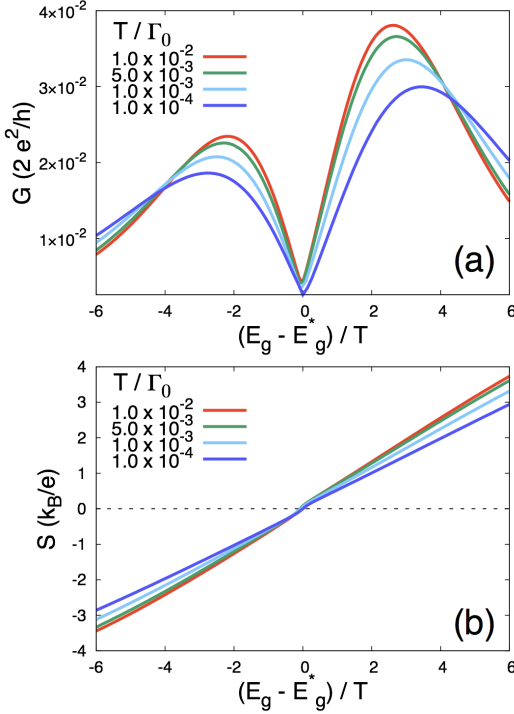


FIG. 2. (color online) Temperature and gate voltage dependence of conductance G (a), and thermopower S (b) when $\mu_0 = 0$. The gate voltage E_g is scaled as $(E_g - E_g^*)/T$, where E_g^* is the gate voltage at the cusp of G .

function of $(E_g - E_g^*)/T$ for several temperatures. The curves of G resemble one another. This means the peak width of the double peaks depends linearly on T . The curves of S are also close to each other; $S \propto (E_g - E_g^*)/T$, and S changes the sign at E_g^* . This means E_g^* gives the boundary between electron-like and hole-like transport. This is in agreement with the fact that E_g^* locates in the VFI regime. Note that the magnitude of S can be large, which is more than $k_B/e \approx 76$ [$\mu\text{V/K}$].

The above results of G and S are explained largely by the shape of $\rho_d(\omega)$. When $U = 0$,

$$\rho_d(\omega) = \frac{-1}{\pi} \text{Im} \frac{1}{\omega - E_g + i\Gamma_0(\omega/D)}. \quad (7)$$

To adjust the QD level shift due to U , we replace E_g with $E_g - E_g^*$. When $U = 0$, the peak width of $\rho_d(\omega)$ is smaller than T , since $D/\Gamma_0 > 1$. It is valid for the present model. Then $\rho_d(\omega)$ can be approximated by a Dirac delta function, $\rho_d(\omega) \sim \delta(\omega - (E_g - E_g^*))$, so that G is determined by the remaining part of the integrand in Eq. (6), $|\omega|f'(\omega)$. This factor explains $G \propto |E_g - E_g^*|$ and the width of the double peak structure. The line shape of S is explained as follows: $I_1(T) \propto |E_g - E_g^*|(E_g - E_g^*)$ near $E_g = E_g^*$, resulting in $S \propto (E_g - E_g^*)/T$. The magnitude of S can be the order of k_B/e since $f'(\omega)$ is finite when $|E_g - E_g^*| \sim T$.

Doped system.— Next we consider the case when the Fermi level is away from the Dirac point; $\mu_0 \neq 0$. Since

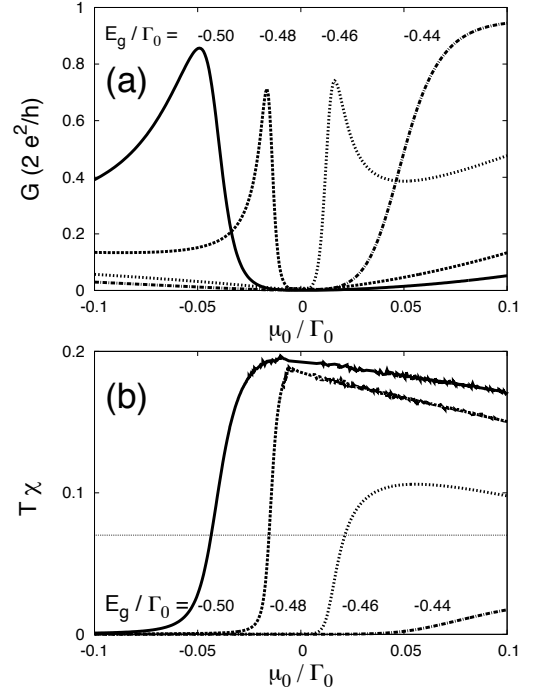


FIG. 3. Conductance G (a), and impurity moment $T\chi$ (b) versus shift of the Fermi level away from the Dirac point μ_0 at $T/\Gamma_0 = 1.0 \times 10^{-4}$. For a free 1/2 spin, $T\chi = 1/4$. The values of E_g are indicated in the figures. The dotted line in (b) indicates $T_K\chi(T_K) = 0.07$.

$\Gamma(\omega)$ is finite at $\omega = 0$, the Kondo effect is active. As a result a clear sign of the transition between the ASC and LM states will appear by tuning external voltages [8, 13].

In Fig. 3, G and the impurity moment $T\chi$ are plotted as a function of μ_0 . The values of E_g are indicated in the figures; two of them are below E_g^* , and two of them above E_g^* . In three of them, G shows a sharp peak. The peak height is about $2e^2/h$. This result is in contrast with the one in Fig. 1(a). When μ_0 is negative and large, $T\chi$ is almost zero. This means that the impurity is screened by the Kondo effect. This corresponds to the ACS state. As μ_0 increases, $T\chi$ increases sharply, where the system moves to the LM state. The sharp peak of G appears at the boundary of the transition of those two states. The Kondo temperature T_K can be defined through $T\chi$; $T_K\chi(T_K) = 0.0701$ [44, 45]. Here we adopt this definition of T_K and draw a line in Fig. 3(b) at $T\chi = 0.07$. Since T_K depends on μ_0 , $T_K(\mu_0) = T$ at the intersection of the line and the curves. The peak structure of G can be associated with the transition at $T \simeq T_K$. Thus $G(\mu_0)$ brings a clear evidence of the transition between the ASC and LM states.

In Fig. 4, G and S are plotted as a function of μ_0 when $E_g/\Gamma_0 = -0.48$ at several temperatures. As the temperature increases, G decreases monotonically. This can be understood by the suppression of the Kondo effect

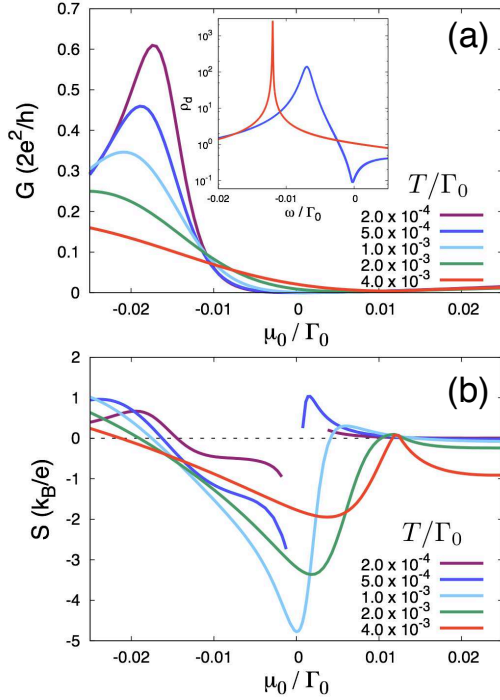


FIG. 4. (color online) Conductance G (a), and thermopower S (b) versus μ_0 for several temperatures and $E_g/\Gamma_0 = -0.48$. Inset (a): $\rho_d(\omega)$ for $\mu_0 = 0$ (blue) and $\mu_0 = 1.2 \times 10^{-2}$ (red), where the dip of S appears, at $T/\Gamma_0 = 4.0 \times 10^{-3}$.

due to the temperature. In the vicinity of the peak of G , S changes its sign. In the ASC state, the Kondo resonant state locates above the Fermi level, whereas in the LM state, the impurity level is below the Fermi level. Thus the sign change of S reflects the transition between two states.

We add two comments on the results of S . First, around $\mu_0 = 0$, S changes the sign for low temperatures, and this change disappears for high temperatures [46]. In

this case, a dip of $\rho_d(\omega)$ induced by the pseudogap crosses the Fermi level as shown by the blue line in the inset of Fig. 4(a). This dip is symmetric around $\omega = 0$. The asymmetry of the dip becomes evident as ω is away from zero. At low temperatures, the crossing of the dip at the Fermi level results in the change the sign of S . At high temperatures, where the asymmetry of $\rho_d(\omega)$ is captured, S remains negative. Second, around $\mu_0/\Gamma_0 = 1.2 \times 10^{-2}$, a clear dip in S appears for high temperatures. This is the place where $\rho_d(\omega)$ shows the critical sharp peak as in Fig. 1(b), at $\omega = -\mu_0$.

We have shown that S can be more than k_B/e , which is dissimilar to the conventional Kondo system [38]. The figure of merit, $ZT = S^2GT/\kappa$, where κ is the thermal conductivity, describes the efficiency of thermoelectric materials [32], and it can be calculated using the Landauer formula approach, where $\kappa = [I_2(T) - I_1(T)^2/I_0(T)]/T$ [35, 43]. Within the present model, $ZT \gtrsim 1$, for wide range of parameter values of T , E_g , and μ_0 , and sometimes ZT becomes more than 10. Thus the pseudogap Kondo system is interesting not only from the point of view of the impurity quantum phase transition, but also for its thermoelectric properties.

In summary, we have investigated the conductance and the thermopower through a QD between Dirac fermions. The pseudogap tunneling coupling between the QD and electrodes suppresses the conductance for undoped electrodes. For doped electrodes, the conductance shows a peak structure which signifies the transition between the ASC and LM states. The thermopower can be more than k_B/e for both doped and undoped cases.

ACKNOWLEDGMENTS

The author thanks Y. Avishai, A. Golub, T. Nakanishi, and Y. Takane for fruitful discussion and comments in various occasions. He also acknowledges the support from JSPS and JST.

-
- [1] A. H. Castro Neto, F. Guinea, N. M. R. Peres, K. S. Novoselov, and A. K. Geim, *Rev. Mod. Phys.*, **81**, 109 (2009).
 - [2] C. Stampfer, J. Güttinger, F. Molitor, D. Graf, T. Ihn, and K. Ensslin, *Appl. Phys. Lett.*, **92**, 012102 (2008).
 - [3] L. A. Ponomarenko, F. Schedin, M. I. Katsnelson, R. Yang, E. W. Hill, K. S. Novoselov, and A. K. Geim, *Science*, **320**, 356 (2008).
 - [4] S. Moriyama, D. Tsuya, E. Watanabe, S. Uji, M. Shimizu, T. Mori, T. Yamaguchi, and K. Ishibashi, *Nano Lett.*, **9**, 2891 (2009).
 - [5] J. Güttinger, T. Frey, C. Stampfer, T. Ihn, and K. Ensslin, *Phys. Rev. Lett.*, **105**, 116801 (2010).
 - [6] D. Goldhaber-Gordon, H. Shtrikman, D. Mahalu, D. Abusch-Magder, U. Meirav, and M. A. Kastner, *Nature*, **391**, 156 (1998).
 - [7] S. M. Cronenwett, T. H. Oosterkamp, and L. P. Kouwenhoven, *Science*, **281**, 540 (1998).
 - [8] K. Sengupta and G. Baskaran, *Phys. Rev. B*, **77**, 045417 (2008).
 - [9] B. Uchoa, L. Yang, S. W. Tsai, N. M. R. Peres, and A. H. Castro Neto, *Phys. Rev. Lett.*, **103**, 206804 (2009).
 - [10] P. S. Cornaglia, G. Usaj, and C. A. Balseiro, *Phys. Rev. Lett.*, **102**, 046801 (2009).
 - [11] H.-B. Zhuang, Q.-f. Sun, and X. C. Xie, *Europhys. Lett.*, **86**, 58004 (2009).
 - [12] T. O. Wehling, A. V. Balatsky, M. I. Katsnelson, A. I. Lichtenstein, and A. Rosch, *Phys. Rev. B*, **81**, 115427 (2010).
 - [13] M. Vojta, L. Fritz, and R. Bulla, *Europhys. Lett.*, **90**, 27006 (2010).
 - [14] B. Uchoa, T. G. Rappoport, and A. H. Castro Neto,

- Phys. Rev. Lett., **106**, 016801 (2011); **106**, 159901(E) (2011).
- [15] J.-H. Chen, L. Li, W. G. Cullen, E. D. Williams, and M. S. Fuhrer, Nature Phys., **7**, 535 (2011).
 - [16] Y. Xia, D. Qian, D. Hsieh, L. Wray, A. Pal, H. Lin, A. Bansil, D. Grauer, Y. S. Hor, R. J. Cava, and M. Z. Hasan, Nature Physics, **5**, 398 (2009).
 - [17] D. Hsieh, Y. Xia, D. Qian, L. Wray, J. H. Dil, F. Meier, J. Osterwalder, L. Patthey, J. G. Checkelsky, N. P. Ong, A. V. Fedorov, H. Lin, A. Bansil, D. Grauer, Y. S. Hor, R. J. Cava, and M. Z. Hasan, Nature, **460**, 1101 (2009).
 - [18] D. Hsieh, Y. Xia, D. Qian, L. Wray, F. Meier, J. H. Dil, J. Osterwalder, L. Patthey, A. V. Fedorov, H. Lin, A. Bansil, D. Grauer, Y. S. Hor, R. J. Cava, and M. Z. Hasan, Phys. Rev. Lett., **103**, 146401 (2009).
 - [19] Y. L. Chen, J. G. Analytis, J.-H. Chu, Z. K. Liu, S.-K. Mo, X. L. Qi, H. J. Zhang, D. H. Lu, X. Dai, Z. Fang, S. C. Zhang, I. R. Fisher, Z. Hussain, and Z.-X. Shen, Science, **325**, 178 (2009).
 - [20] H. Zhang, C.-X. Liu, X.-L. Qi, X. Dai, Z. Fang, and S.-C. Zhang, Nature Phys., **5**, 438 (2009).
 - [21] Q. Liu, C.-X. Liu, C. Xu, X.-L. Qi, and S.-C. Zhang, Phys. Rev. Lett., **102**, 156603 (2009).
 - [22] M.-T. Tran and K.-S. Kim, Phys. Rev. B, **82**, 155142 (2010).
 - [23] R. Žitko, Phys. Rev. B, **81**, 241414 (2010).
 - [24] X.-Y. Feng, W.-Q. Chen, J.-H. Gao, Q.-H. Wang, and F.-C. Zhang, Phys. Rev. B, **81**, 235411 (2010).
 - [25] D. Withoff and E. Fradkin, Phys. Rev. Lett., **64**, 1835 (1990).
 - [26] C. R. Cassanello and E. Fradkin, Phys. Rev. B, **53**, 15079 (1996); **56**, 11246 (1997).
 - [27] C. Gonzalez-Buxton and K. Ingersent, Phys. Rev. B, **54**, R15614 (1996); **57**, 14254 (1998).
 - [28] R. Bulla, Th. Pruschke, and A. C. Hewson, J. Phys. Condens. Matter, **9**, 10463 (1997).
 - [29] L. Fritz and M. Vojta, Phys. Rev. B, **70**, 214427 (2004).
 - [30] M. Vojta and L. Fritz, Phys. Rev. B, **70**, 094502 (2004).
 - [31] T. Kanao, H. Matsuura, and M. Ogata, J. Phys. Soc. Jpn., **81**, 063709 (2012).
 - [32] Y. Dubi and M. Di Ventra, Rev. Mod. Phys., **83**, 131 (2011).
 - [33] J. Kondo, Prog. Theor. Phys., **34**, 372 (1965).
 - [34] D. Boese and R. Fazio, Europhys. Lett., **56**, 576 (2001).
 - [35] B. Dong and X. L. Lei, J. Phys. Condens. Matter, **14**, 11747 (2002).
 - [36] R. Scheibner, H. Buhmann, D. Reuter, M. N. Kiselev, and L. W. Molenkamp, Phys. Rev. Lett., **95**, 176602 (2005).
 - [37] P. Coleman, Phys. Rev. B, **29**, 3035 (1984).
 - [38] N. E. Bickers, Rev. Mod. Phys., **59**, 845 (1987).
 - [39] N. S. Wingreen and Y. Meir, Phys. Rev. B, **49**, 11040 (1994).
 - [40] M. Vojta, Phys. Rev. Lett., **87**, 097202 (2001).
 - [41] For the K' point, the off-diagonal elements of M are replaced by their complex conjugates.
 - [42] S. E. Barnes, J. Phys. F, **6**, 1375 (1976); **7**, 2637 (1977).
 - [43] J. Liu, Q.-f. Sun, and X. C. Xie, Phys. Rev. B, **81**, 245323 (2010).
 - [44] H. R. Krishna-murthy, J. W. Wilkins, and K. G. Wilson, Phys. Rev. B, **21**, 1003 (1980).
 - [45] L. G. G. V. Dias da Silva, N. Sandler, P. Simon, K. Ingersent, and S. E. Ulloa, Phys. Rev. Lett., **102**, 166806 (2009).
 - [46] The gap in the curves of S for low temperatures means that we do not achieve good convergence of the numerical calculation.